Theoretical background of two high precision experiments

1. HD^+ spectroscopy
2. HF splitting in muonic hydrogen

Precision spectroscopy of hydrogen molecular ions

S. Schiller (University of Dusseldorf)
V.I. Korobov (JINR, Dubna)
D. Bakalov (INRNE, Sofia)

HD^+ spectroscopy: history

- An experimental activity of S. Schiller's group (University of Duesseldorf) since 15 years
- Constantly increasing accuracy:

  2006: ~100 kHz

  2014: <10 kHz
- initially: HD^+ in Coulomb crystals

  now: single trapped HD^+ in Lamb-Dicke regime

HD^+ spectroscopy: goals

- Determining the values of fundamental constants with improved accuracy:

  m_e/m_p, m_e/m_d, α, Ry, …

- Developing high stability standards of time, testing the time variability of the constants:

  $\delta\nu/\nu < 5.10^{-18}$

Systematic effects in HD^+

- Shifts, related to the measurement (light shift, 2nd order Doppler shift, ...) - under control
- External field effects:

  - Zeeman shift

  - d.c. Stark shift

  - electric quadrupole shift

  - a.c. Stark shift, BBR shift

Effective Hamiltonian

$$
\begin{aligned}
H^{\mathrm{eff}} = {} & E_1(\mathbf{L}\cdot\mathbf{S}_e) + E_2(\mathbf{L}\cdot\mathbf{S}_p) + E_3(\mathbf{L}\cdot\mathbf{S}_d) \\
& + E_4(\mathbf{S}_p\cdot\mathbf{S}_e) + E_5(\mathbf{S}_d\cdot\mathbf{S}_e) \\
& + 2E_6\left(\mathbf{L}^2(\mathbf{S}_p\cdot\mathbf{S}_e) - 3(\mathbf{L}\cdot\mathbf{S}_e)(\mathbf{L}\cdot\mathbf{S}_p)\right) \\
& + 2E_7\left(\mathbf{L}^2(\mathbf{S}_d\cdot\mathbf{S}_e) - 3(\mathbf{L}\cdot\mathbf{S}_e)(\mathbf{L}\cdot\mathbf{S}_d)\right) \\
& + 2E_8\left(\mathbf{L}^2(\mathbf{S}_p\cdot\mathbf{S}_d) - 3(\mathbf{L}\cdot\mathbf{S}_p)(\mathbf{L}\cdot\mathbf{S}_d)\right) \\
& + E_9\left(\mathbf{L}^2\mathbf{S}_d^2 - \frac{3}{2}(\mathbf{L}\cdot\mathbf{S}_d) - 3(\mathbf{L}\cdot\mathbf{S}_d)^2\right), \\
& + E_{10}(\mathbf{L}\cdot\mathbf{B}) + E_{11}(\mathbf{S}_p\cdot\mathbf{B}) + E_{12}(\mathbf{S}_d\cdot\mathbf{B}) \\
& + E_{13}(\mathbf{S}_e\cdot\mathbf{B}) + \sqrt{\frac{3}{2}}\,E_{14}\left(Q\cdot(\mathbf{L}\otimes\mathbf{L})^{(2)}\right) \\
& + E_{15}\,\mathbf{E}^2 + E_{16}\left((\mathbf{L}\cdot\mathbf{E})^2 - \frac{1}{3}\mathbf{L}^2\mathbf{E}^2\right)
\end{aligned}
$$

Hyperfine interactions

$$
\begin{aligned}
H^{\text{eff}} = & E_1(\mathbf{L}\cdot\mathbf{S}_e) + E_2(\mathbf{L}\cdot\mathbf{S}_p) + E_3(\mathbf{L}\cdot\mathbf{S}_d) \\
&+E_4(\mathbf{S}_p\cdot\mathbf{S}_e) + E_5(\mathbf{S}_d\cdot\mathbf{S}_e) \\
&+2E_6\left(\mathbf{L}^2(\mathbf{S}_p\cdot\mathbf{S}_e) - 3(\mathbf{L}\cdot\mathbf{S}_e)(\mathbf{L}\cdot\mathbf{S}_p)\right) \\
&+2E_7\left(\mathbf{L}^2(\mathbf{S}_d\cdot\mathbf{S}_e) - 3(\mathbf{L}\cdot\mathbf{S}_e)(\mathbf{L}\cdot\mathbf{S}_d)\right) \\
&+2E_8\left(\mathbf{L}^2(\mathbf{S}_p\cdot\mathbf{S}_d) - 3(\mathbf{L}\cdot\mathbf{S}_p)(\mathbf{L}\cdot\mathbf{S}_d)\right) \\
&+E_9\left(\mathbf{L}^2\mathbf{S}_d^2 - \frac{3}{2}(\mathbf{L}\cdot\mathbf{S}_d) - 3(\mathbf{L}\cdot\mathbf{S}_d)^2\right), \\
&+E_{10}(\mathbf{L}\cdot\mathbf{B}) + E_{11}(\mathbf{S}_p\cdot\mathbf{B}) + E_{12}(\mathbf{S}_d\cdot\mathbf{B}) \\
&+E_{13}(\mathbf{S}_e\cdot\mathbf{B}) + \sqrt{\frac{3}{2}}E_{14}\left(Q\cdot(\mathbf{L}\otimes\mathbf{L})^{(2)}\right) \\
&+E_{15}\,\mathbf{E}^2 + E_{16}\left((\mathbf{L}\cdot\mathbf{E})^2 - \frac{1}{3}\mathbf{L}^2\mathbf{E}^2\right)
\end{aligned}
$$

Zeeman shift

$$
\begin{aligned}
H^{\rm eff} = {} & E_1(\mathbf{L}\cdot\mathbf{S}_e) + E_2(\mathbf{L}\cdot\mathbf{S}_p) + E_3(\mathbf{L}\cdot\mathbf{S}_d) \\
& + E_4(\mathbf{S}_p\cdot\mathbf{S}_e) + E_5(\mathbf{S}_d\cdot\mathbf{S}_e) \\
& + 2E_6\left(\mathbf{L}^2(\mathbf{S}_p\cdot\mathbf{S}_e) - 3(\mathbf{L}\cdot\mathbf{S}_e)(\mathbf{L}\cdot\mathbf{S}_p)\right) \\
& + 2E_7\left(\mathbf{L}^2(\mathbf{S}_d\cdot\mathbf{S}_e) - 3(\mathbf{L}\cdot\mathbf{S}_e)(\mathbf{L}\cdot\mathbf{S}_d)\right) \\
& + 2E_8\left(\mathbf{L}^2(\mathbf{S}_p\cdot\mathbf{S}_d) - 3(\mathbf{L}\cdot\mathbf{S}_p)(\mathbf{L}\cdot\mathbf{S}_d)\right) \\
& + E_9\left(\mathbf{L}^2\mathbf{S}_d^2 - \frac{3}{2}(\mathbf{L}\cdot\mathbf{S}_d) - 3(\mathbf{L}\cdot\mathbf{S}_d)^2\right), \\
& + E_{10}(\mathbf{L}\cdot\mathbf{B}) + E_{11}(\mathbf{S}_p\cdot\mathbf{B}) + E_{12}(\mathbf{S}_d\cdot\mathbf{B}) \\
& + E_{13}(\mathbf{S}_e\cdot\mathbf{B}) + \sqrt{\frac{3}{2}}\,E_{14}\left(Q\cdot(\mathbf{L}\otimes\mathbf{L})^{(2)}\right) \\
& + E_{15}\,\mathbf{E}^2 + E_{16}\left((\mathbf{L}\cdot\mathbf{E})^2 - \frac{1}{3}\mathbf{L}^2\mathbf{E}^2\right)
\end{aligned}
$$

Zeeman shift

$$H_{\text{eff}}^{\text{tot}} = H_{\text{eff}}^{\text{hfs}} + E_{10}(\mathbf{L} \cdot \mathbf{B}) + E_{11}(\mathbf{S}_p \cdot \mathbf{B}) + E_{12}(\mathbf{S}_d \cdot \mathbf{B}) + E_{13}(\mathbf{S}_e \cdot \mathbf{B}),$$

$$E_{11} = -\frac{e\mu_p}{M_p c} = -4.2577 \text{ kHz G}^{-1},$$

$$E_{12} = -\frac{e\mu_d}{2M_d c} = -0.6536 \text{ kHz G}^{-1},$$

$$E_{13} = \frac{e\mu_e}{M_e c} = 2.8025 \text{ MHz G}^{-1}.$$

$$E_{10} = -\mu_B \sum_i \frac{Z_i M_e}{M_i} \frac{\langle vL \| \mathbf{L}_i \| vL \rangle}{\sqrt{L(L+1)(2L+1)}}.$$

Zeeman shift

$$(\Delta E^{vLnJ_z}(B) - \Delta E^{vLnJ_z}(0))/h \approx t^{vLn} \cdot J_z \cdot B + \left(q^{vLn} + r^{vLn} \cdot J_z^2\right) \cdot B^2,$$

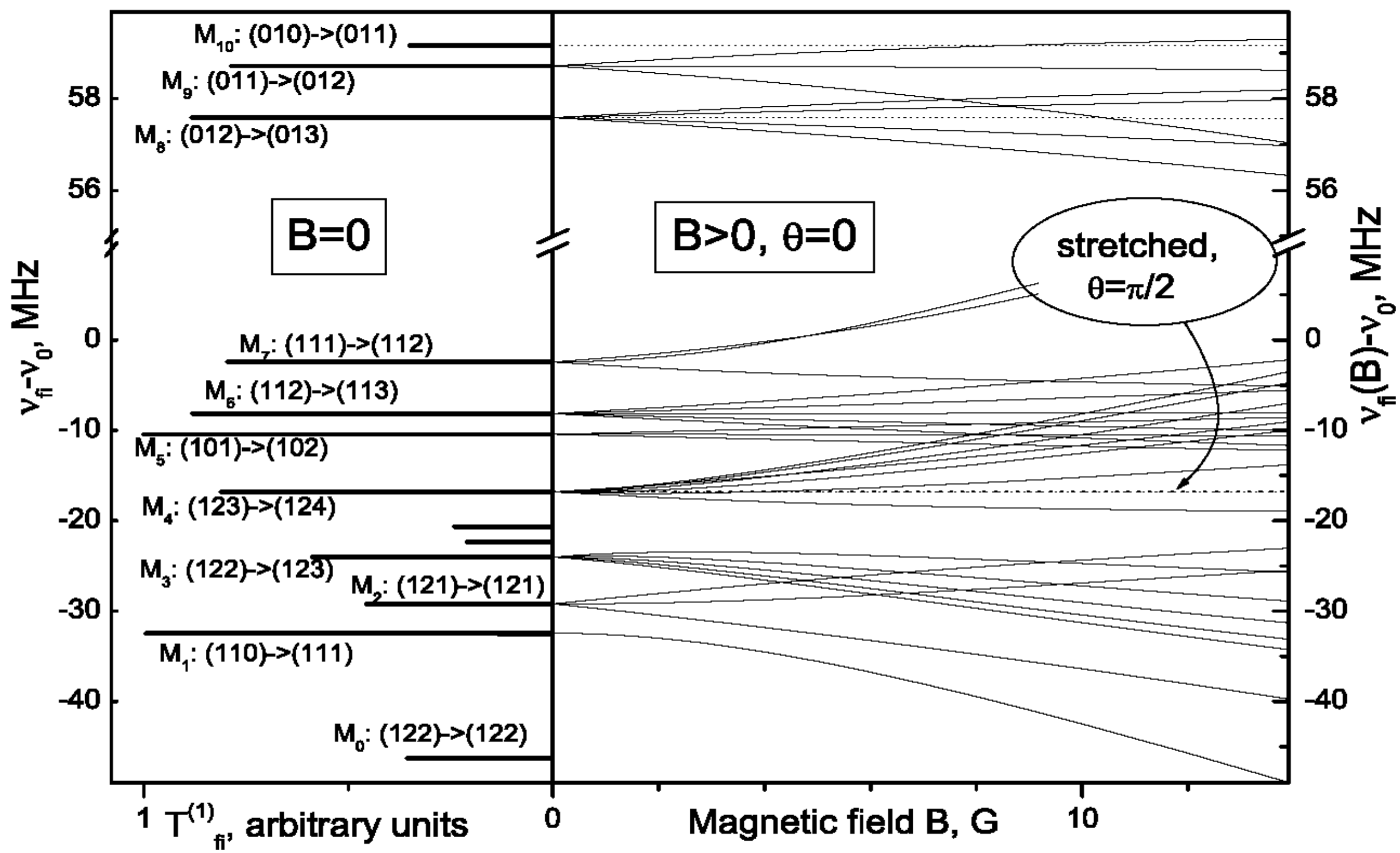

Electric quadrupole shift

$$
\begin{aligned}
H^{\text{eff}} = {} & E_1(\mathbf{L}\cdot\mathbf{S}_e) + E_2(\mathbf{L}\cdot\mathbf{S}_p) + E_3(\mathbf{L}\cdot\mathbf{S}_d) \\
& + E_4(\mathbf{S}_p\cdot\mathbf{S}_e) + E_5(\mathbf{S}_d\cdot\mathbf{S}_e) \\
& + 2E_6\left(\mathbf{L}^2(\mathbf{S}_p\cdot\mathbf{S}_e) - 3(\mathbf{L}\cdot\mathbf{S}_e)(\mathbf{L}\cdot\mathbf{S}_p)\right) \\
& + 2E_7\left(\mathbf{L}^2(\mathbf{S}_d\cdot\mathbf{S}_e) - 3(\mathbf{L}\cdot\mathbf{S}_e)(\mathbf{L}\cdot\mathbf{S}_d)\right) \\
& + 2E_8\left(\mathbf{L}^2(\mathbf{S}_p\cdot\mathbf{S}_d) - 3(\mathbf{L}\cdot\mathbf{S}_p)(\mathbf{L}\cdot\mathbf{S}_d)\right) \\
& + E_9\left(\mathbf{L}^2\mathbf{S}_d^2 - \frac{3}{2}(\mathbf{L}\cdot\mathbf{S}_d) - 3(\mathbf{L}\cdot\mathbf{S}_d)^2\right), \\
& + E_{10}(\mathbf{L}\cdot\mathbf{B}) + E_{11}(\mathbf{S}_p\cdot\mathbf{B}) + E_{12}(\mathbf{S}_d\cdot\mathbf{B}) \\
& + E_{13}(\mathbf{S}_e\cdot\mathbf{B}) + \boxed{\sqrt{\frac{3}{2}}\,E_{14}\left(Q\cdot(\mathbf{L}\otimes\mathbf{L})^{(2)}\right)} \\
& + E_{15}\,\mathbf{E}^2 + E_{16}\left((\mathbf{L}\cdot\mathbf{E})^2 - \frac{1}{3}\mathbf{L}^2\mathbf{E}^2\right)
\end{aligned}
$$

Electric quadrupole shift

$$\Delta H_Q = -\frac{1}{3}\Theta_C \cdot Q(\mathbf{R}_C),$$

$$Q(\mathbf{R}_C)_{ij} = -(\partial^2/\partial x_i \partial x_j)U(\mathbf{x})|_{\mathbf{x}=\mathbf{R}_C}.$$

$$(\Theta_C)_{ij} = \frac{3}{2}e\left(a_0\left(R_iR_j - \frac{\delta_{ij}}{3}\mathbf{R}^2\right) + a_1\left(\frac{R_ir_j + r_iR_j}{2} - \frac{\delta_{ij}}{3}\mathbf{R}\cdot\mathbf{r}\right) - a_2\left(r_ir_j - \frac{\delta_{ij}}{3}\mathbf{r}^2\right)\right),$$

$$\Delta E^{vLFSJJ_z}_{\mathrm{Q,diag}} = \sqrt{\frac{3}{2}}E_{14}(v,L)Q_{zz}\langle vLFSJJ_z|L_z^2 - \frac{1}{3}\mathbf{L}^2|vLFSJJ_z\rangle.$$

dc Stark shift

$$
\begin{aligned}
H^{\text{eff}} = &\, E_1(\mathbf{L}\cdot\mathbf{S}_e) + E_2(\mathbf{L}\cdot\mathbf{S}_p) + E_3(\mathbf{L}\cdot\mathbf{S}_d) \\
&+E_4(\mathbf{S}_p\cdot\mathbf{S}_e) + E_5(\mathbf{S}_d\cdot\mathbf{S}_e) \\
&+2E_6\left(\mathbf{L}^2(\mathbf{S}_p\cdot\mathbf{S}_e) - 3(\mathbf{L}\cdot\mathbf{S}_e)(\mathbf{L}\cdot\mathbf{S}_p)\right) \\
&+2E_7\left(\mathbf{L}^2(\mathbf{S}_d\cdot\mathbf{S}_e) - 3(\mathbf{L}\cdot\mathbf{S}_e)(\mathbf{L}\cdot\mathbf{S}_d)\right) \\
&+2E_8\left(\mathbf{L}^2(\mathbf{S}_p\cdot\mathbf{S}_d) - 3(\mathbf{L}\cdot\mathbf{S}_p)(\mathbf{L}\cdot\mathbf{S}_d)\right) \\
&+E_9\left(\mathbf{L}^2\mathbf{S}_d^2 - \frac{3}{2}(\mathbf{L}\cdot\mathbf{S}_d) - 3(\mathbf{L}\cdot\mathbf{S}_d)^2\right), \\
&+E_{10}(\mathbf{L}\cdot\mathbf{B}) + E_{11}(\mathbf{S}_p\cdot\mathbf{B}) + E_{12}(\mathbf{S}_d\cdot\mathbf{B}) \\
&+E_{13}(\mathbf{S}_e\cdot\mathbf{B}) + \sqrt{\frac{3}{2}}E_{14}\left(Q\cdot(\mathbf{L}\otimes\mathbf{L})^{(2)}\right) \\
&+E_{15}\,\mathbf{E}^2 + E_{16}\left((\mathbf{L}\cdot\mathbf{E})^2 - \frac{1}{3}\mathbf{L}^2\mathbf{E}^2\right)
\end{aligned}
$$

dc Stark shift

$E_{15} = -\alpha_s/2, \quad E_{16} = -\alpha_t$

$$\alpha_s = \frac{1}{3}(a_+ + a_0 + a_-),$$

$$\alpha_t = -\frac{a_+}{2(L+1)(2L+3)} + \frac{a_0}{2L(L+1)} - \frac{a_-}{2L(2L-1)}.$$

$$a_+ = \frac{2}{2L+1} \sum_p \frac{\langle vL \| \mathbf{d} \| p(L+1) \rangle \langle p(L+1) \| \mathbf{d} \| vL \rangle}{E_0 - E_p},$$

$$a_0 = -\frac{2}{2L+1} \sum_p \frac{\langle vL \| \mathbf{d} \| pL \rangle \langle pL \| \mathbf{d} \| vL \rangle}{E_0 - E_p},$$

$$a_- = \frac{2}{2L+1} \sum_p \frac{\langle v\, L \| \mathbf{d} \| p\, (L-1) \rangle \langle p\, (L-1) \| \mathbf{d} \| v\, L \rangle}{E_0 - E_p}$$

ac Stark & BBR shift

$$\Delta E_{\mathrm{BBR}}(m,T) = -\frac{1}{2}\int_0^\infty \alpha_s(m,\omega)\mathcal{E}_{\mathrm{BBR}}(T,\omega)^2 d\omega,$$

To a good approximation: independent of the hyperfine state, but dependent on the temperature.

Particularly stable transitions

Among the large amount of HF transitions –

many with overall shift at typical external field intensities suppressed to ~10-80 Hz including:

- E1 dipole transitions
- Two-photon transitions
- M1 HF transition

Composite frequency

- For each HF state: the shift of the energy level

  $\Delta E_k = \Delta E_k(B, E, Q, \theta)$

- For each HF transition: the shift of the frequency $\Delta\nu(B_x, B_y, B_z, E_x, E_y, E_z, Q_{xx}, \ldots, Q_{zz})$
- Denote the relevant parameters by X_j

  $\Delta\nu_k(X_j) = \Sigma_j (\partial\nu_k/\partial X_j)\, X_j$ are all known!

Then:

Composite frequency

- Consider $\nu_c=\Sigma_k\, c_k\, \nu_k$

- The coefficients c_k may be selected in a way that $\partial\nu_c/\partial X_j$ is independent of X_j:

$$\Sigma_k\, (\partial\nu_k/\partial X_j)\, c_k=0,\ k=1,\ldots,K;\ j=1,\ldots J,\ K>J$$

Composite frequency: example

(v', L') upper	(v, L) lower	F'	S'	J'	J'_z	F	S	J	J_z	δf_0 [MHz]	Δf_{Z2} [Hz]	Δf_{EQ} [Hz]	$\Delta f_S^{(t)}$ [mHz]	$\Delta f_S^{(l)}$ [mHz]	Δf_{BB} [mHz]	σ_{BB,T_0} [mHz]	β_i
HD^+; $f_c = 147.78$ THz, $\sigma_{\mathrm{syst},f_c}/f_c = 5.4 \times 10^{-18}$, $\Delta f_{\mathrm{BB},f_c}/f_c = 4.0 \times 10^{-17}$; $(\sigma_{\mathrm{Z2},f_c}, \sigma^{(t)}_{\mathrm{S},f_c}, \sigma^{(l)}_{\mathrm{S},f_c}, \sigma_{\mathrm{EQ},f_c}, \sigma_{\mathrm{BB},f_c})/f_c = (0.6, 0.2, 0.4, 4.8, 2.4) \times 10^{-18}$																	
(3, 2)	(0, 1)	1	1	3	0	1	1	2	0	−3.8	0.008	−1.42	10.3	−24.7	−17.4	−1.8	1
(3, 3)	(0, 2)	1	0	3	0	1	0	2	0	−10.8	0.022	−1.13	1.6	−7.3	−18.3	−1.8	−1.49
(3, 4)	(0, 3)	1	2	4	0	1	2	3	0	−16.0	0.003	−1.49	−2.6	1.0	−18.7	−1.9	−1.67
(3, 4)	(0, 3)	1	1	5	0	1	1	4	0	−8.4	−0.004	−1.22	−1.0	−2.1	−18.7	−1.9	−1.38
(4, 2)	(0, 1)	0	1	1	0	0	1	0	0	59.1	−0.007	−3.67	−19.8	33.6	−24.6	−2.7	0.40
(5, 5)	(0, 4)	0	1	4	0	0	1	3	0	70.8	0.018	−2.15	−4.1	−0.7	−37.3	−4.1	1.37
composite frequency:											0	0	0	0	5.9	0	

Muonic hydrogen hyperfine splitting experiment (FAMU)

A.Vacchi (INFN-Trieste, Italy)

A.Adamczak (IFJ, Krakow, Poland)

D. Bakalov (INRNE, Sofia, Bulgaria)

Why muonic hydrogen atoms?

Two main motives:

1. Unique opportunity for new precision tests of Quantum electrodynamics

2. Investigations of proton e.m. structure

Motive 2: Proton structure

Initially the ideas were (~1980) :

Measurement of the hyperfine splitting (HFS) in the ground state of muonic hydrogen is complementary to the top accuracy ~1970 measurement of the HFS of ordinary H

Two measurements will give the two parameters "Zemach radius" and "polarizability" of proton

$$E^{HFS}=E^{F}(1+\delta^{QED}+\delta^{rec}+\boldsymbol{\delta^{pol}}+\boldsymbol{\delta^{Z}})$$

Motive 2: Proton structure

Updated point of view (since ~2001)

1. Proton polarizability correction δ^{pol} is not related to a single parameter, but is assumed known from phenomenological calculations.
2. The Zemach radius R_Z can be determined from a measurement of E^{HFS} using (tentatively!)

$$R_Z = \left(184.087(xx) - E^{HFS}(exp)\right)/1.281(yy)$$

(xx)~(15), (yy)<10

Motive 2: Proton structure

What are the limitations on the accuracy of R_Z?

$E^F, \delta^{QED}, \delta^{rec}, \ldots$ known or calculable to 10^{-6}

$\delta^{pol} = (0.46 \pm 0.08) \times 10^{-3}$

$\delta^{Z} = (1.0152 \times 2 m_{\mu p} \alpha \mathbf{R_Z}) \approx 8 \times 10^{-3}$

Limit: $0.08 \times 10^{-3} / \delta^{Z} \approx 1\%$

R_Z can be determined to 1% if $\boldsymbol{\delta}_{exp} E^{HFS} < 0.8 \times 10^{-4}$

Proton size (till ~12 years ago)

	charge radius r_{ch}
e^--p scattering & spectroscopy	$r_{ch} = 0.8775(51)$

(the last digits may have changed)

…when people also though of R_Z

	charge radius r_{ch}	Zemach radius R_Z
e^--p scattering & spectroscopy	r_{ch} = 0.8775(51)	R_Z=1.037(16) Dupays&*al*'<u>03</u> R_Z=1.086(12) Friar&Sick'<u>04</u> R_Z=1.047(16) Volotka&*al*'<u>05</u> R_Z=1.045(4) Distler&*al*'<u>11</u>

4 independent results, grouped around the <u>incompatible</u> values 1.04 and 1.09 fm.

2010: proton size puzzle!

	charge radius r_{ch}	Zemach radius R_Z
e^--p scattering & spectroscopy	r_{ch} = 0.8775(51)	R_Z=1.037(16) Dupays&*al*'03 R_Z=1.086(12) Friar&Sick'04 R_Z=1.047(16) Volotka&*al*'05 R_Z=1.045(4) Distler&*al*'11
μ^--p Lamb shift spectroscopy	r_{ch} =0.84089(39)	

7σ

Can R_Z from μ^-p help solve it?

	charge radius r_{ch}	Zemach radius R_Z
e^--p scattering & spectroscopy	r_{ch} = 0.8775(51)	R_Z=1.037(16) Dupays&*al*'03 R_Z=1.086(12) Friar&Sick'04 R_Z=1.047(16) Volotka&*al*'05 R_Z=1.045(4) Distler&*al*'11
μ^--p Lamb shift spectroscopy	r_{ch}=0.84089(39)	Either confirm a e^-p value or admit: e^-p and μ^-p differ **???**

Alternatives: insufficient accuracy

	charge radius r_{ch}	Zemach radius R_Z
e^--p scattering & spectroscopy	$r_{ch} = 0.8775(51)$	R_Z=1.037(16) [Dupays&al'03] R_Z=1.086(12) [Friar&Sick'04] R_Z=1.047(16) [Volotka&*al*'05] R_Z=1.045(4) [Distler&*al*'11]
μ^--p Lamb shift spectroscopy	r_{ch}=0.84089(39)	Very recently: R_Z = 1.082(37) [PSI'12] from HFS of $(\mu^- p)_{2S}$

Present status of FAMU

Key points:

1. Tunable IR laser
2. Multipass cavity
3. Muon source
4. Detecting systems
5. Experimental method

1.Tunable pulsed IR laser at λ=6.8μ

Direct difference frequency generation in non-oxide nonlinear crystals using singlemode Nd:YAG laser and tunable Cr:forsterite laser

Targeted characteristics (L.Stoychev, EOSAM ’14)

- Pulse energy: 5mJ
- Line width: 250 MHz
- Repetition rate: 50 Hz
- Tunability: 3nm

1.Tunable pulsed IR laser at λ=6.8μ

Scheme based on Difference Frequency Generation in which the radiation 1.06μm of a Nd-YAG is mixed with the 1.26μm radiation of Cr-forsterite laser

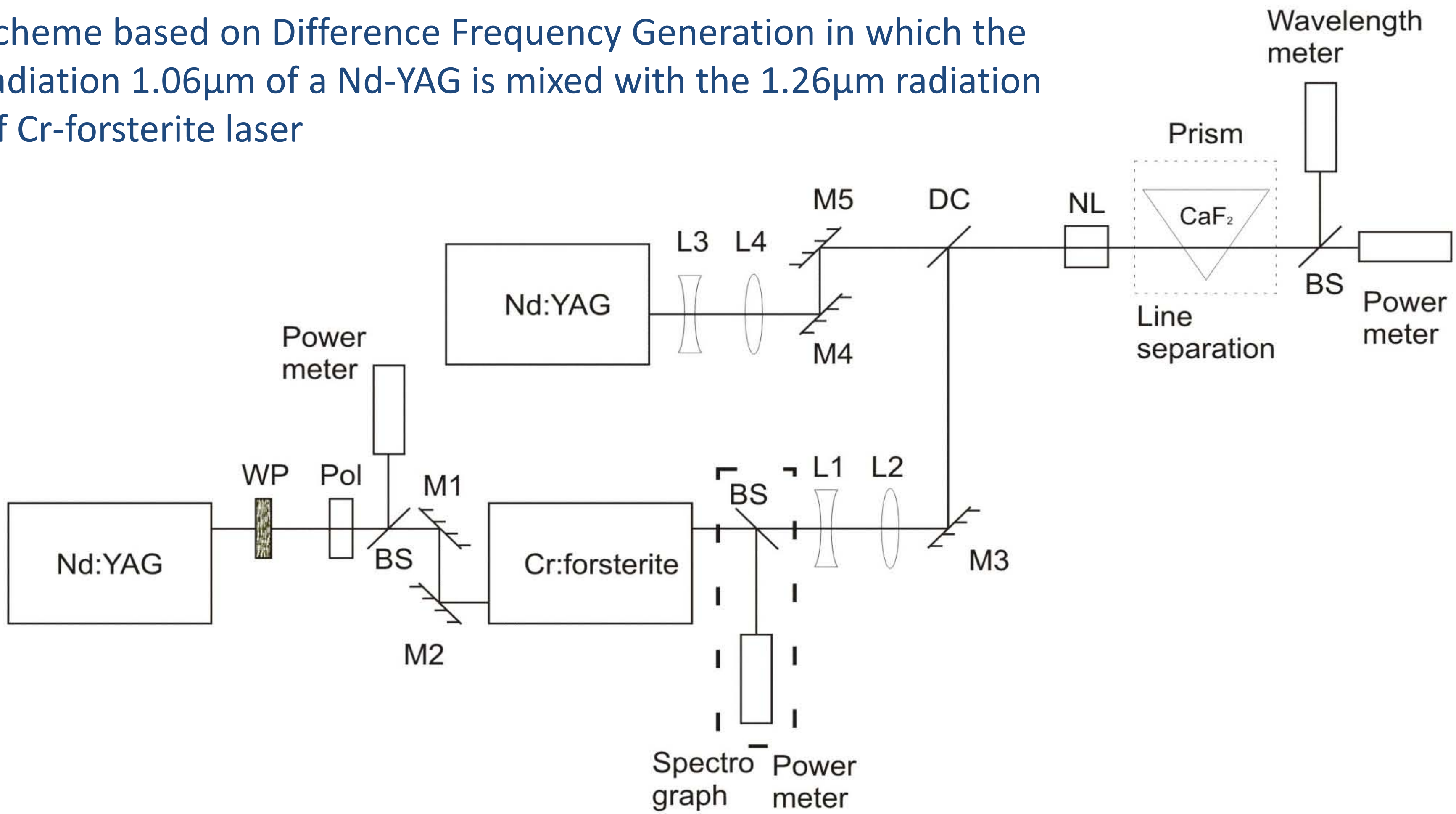

WP - waveplate, Po - polarizer, M1-M5 - mirrors, L1 and L3 - negative lenses, L2 - L4 positive lenses, BS - beamsplitters, DC - dichroic mirror

2. Multi-pass cavity

- Various designs discussed

- Most appropriate: a modification of the multipass cavity of the PSI Lamb shift exp.

  amplification factor: ~2000

3.Pulsed RIKEN/RAL muon source

Main characteristics

Negative muons in the range [20-120] MeV/c

7×10^4 muons/sec at 60 MeV/c

50 Hz repetition rate

Double pulses of 70 ns with 320 ns gap

Beam shape: δ_x=1.08 cm, δ_y=1.19 cm

4. Detecting systems

- HP Ge and LaBr X-ray detectors in the range

  60 – 550 keV

- Efficiency limited by

  - solid angle covered

  - overlapping events

  - …

5. Experimental method

- Physical basis
- Experimental verification
- Monte Carlo simulations
- Estimates of the efficiency

Physical basis of the method

1. A laser pulse of resonance λ_0~6.8μ converts the spin state of (μ^-p) from 1^1S_0 to 1^3S_1
2. (μ^-p) atoms in 1^3S_1 state are collisionally de-excited and accelerated by ~0.12 eV
3. The muons are transferred to heavier gases with an energy-dependent rate
4. λ_0 is recognized by the maximal response in the time distribution of μ-transfer events

Experimental verification needed

Key point:

Is the muon transfer rate to higher-Z atoms in collisions of μp energy dependent at epithermal energies $\epsilon_T < E < \epsilon_T + 0.12$ eV?

Theory: no energy dependence at $E \rightarrow 0$

Experimental eveidences of energy dependent rate of transfer to O and Ar [PSI, 1995]

Preceding experiments

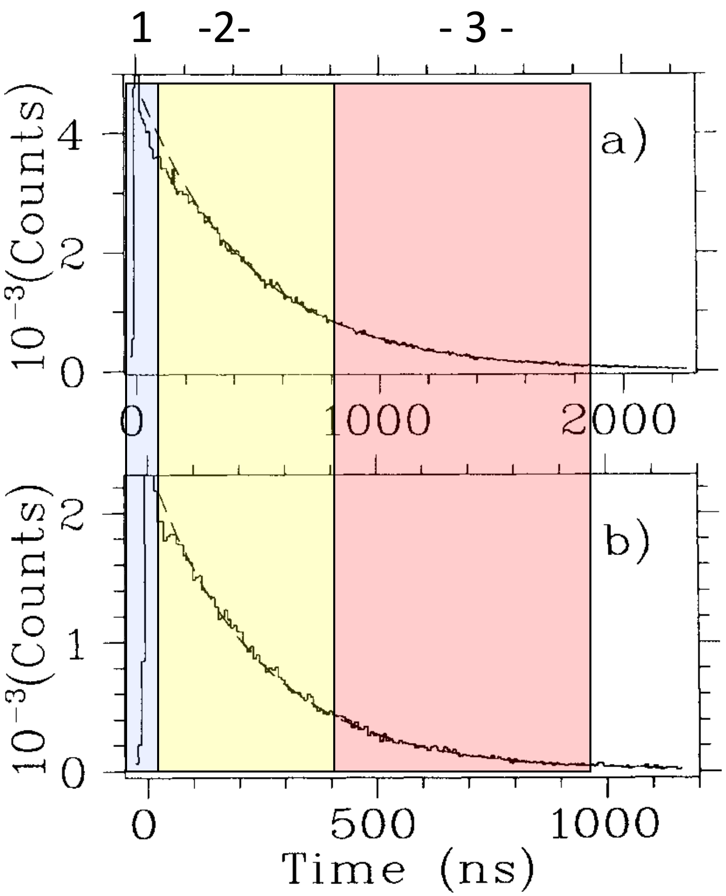

dμ+Ne→μNe+d, R.J.-G., PRA51(95)

Measured: the time distribution of characteristic X-rays

Three time ranges:

1. Prompt peak from direct capture
2. Transfer from epithermic $\mu^{-}p$
3. Transfer from thermalized $\mu^{-}p$

An alternative method proposed

$$\Lambda(T) = \int \lambda(\varepsilon)\rho(\varepsilon)\, d\varepsilon$$

$$\rho(\varepsilon) = \rho_{\mathrm{MB}}(\varepsilon; T) = \rho_0(\varepsilon/\varepsilon_T)/\varepsilon_T \,,$$

$$\rho_0(x) = (2\sqrt{x/\pi})\exp(-x)\,, \quad \varepsilon_T = k_B T$$

$$\Lambda_k = \Lambda(T_k)$$

Λ_k: muon transfer rate measured in completely thermalized gas target at temperature T_k

An alternative method proposed

$$\lambda(\varepsilon) = \sum_{k=1} \Lambda_k P^{(k)}(\varepsilon)$$

$$P^{(k)}(\varepsilon) = \sum_{n=0}^{N-1} \varepsilon^n \frac{4^n}{(2n+1)!} \frac{\partial^n}{\partial z^n} \prod_{j \neq k} \frac{(z - \varepsilon_j)}{(\varepsilon_k - \varepsilon_j)} \bigg|_{z=0}$$

$$\Delta\lambda(\varepsilon)^2 = \sum_{k=1}^{N} (P^{(k)}(\varepsilon))^2 \Delta_k^2 .$$

Uncertainty of the extracted rate

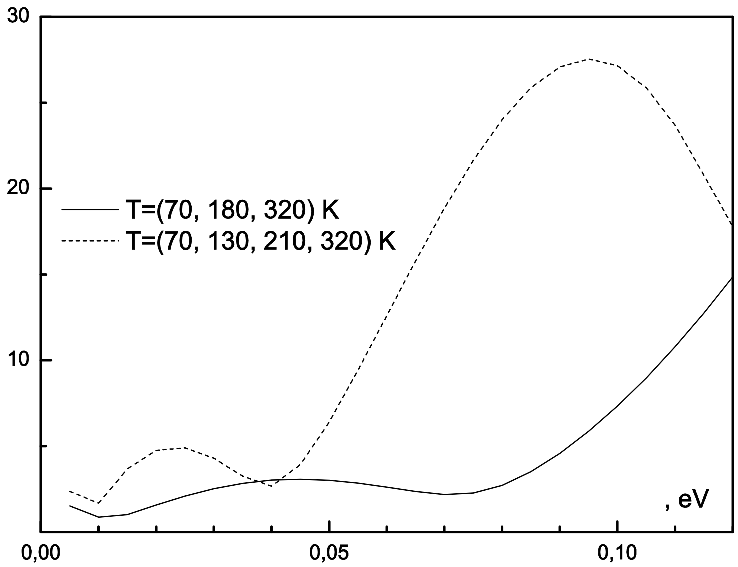

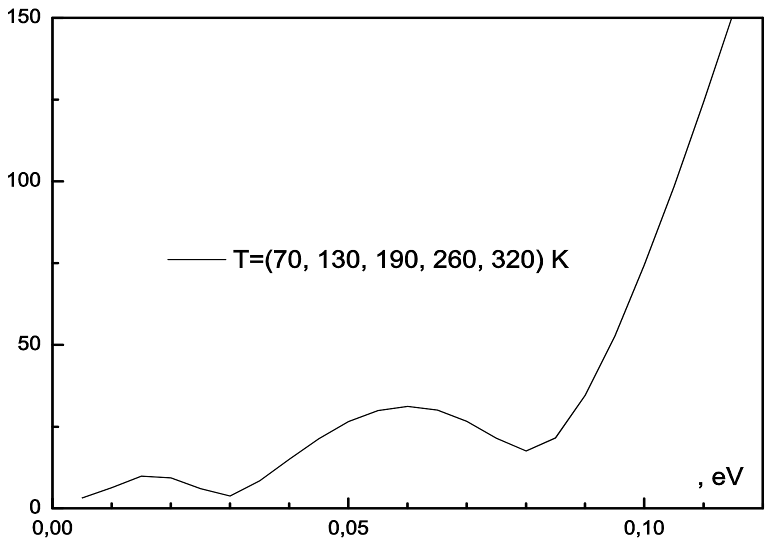

Experimental verification started!

First test run at RIKEN/RAL earlier this year in the frame of FAMU experiment (INFN):

Tested target, detectors, beam adjustments

Run at 300K, 35 Atm, various target gas mixtures (H_2, H_2+O_2, H_2+CO_2, H_2+Ar)

Next runs: measurements at different temperatures in the range [70-400]K

HPGe through spectroscopic preamplifier Spectrum evidencing the 134 KeV muonic lines

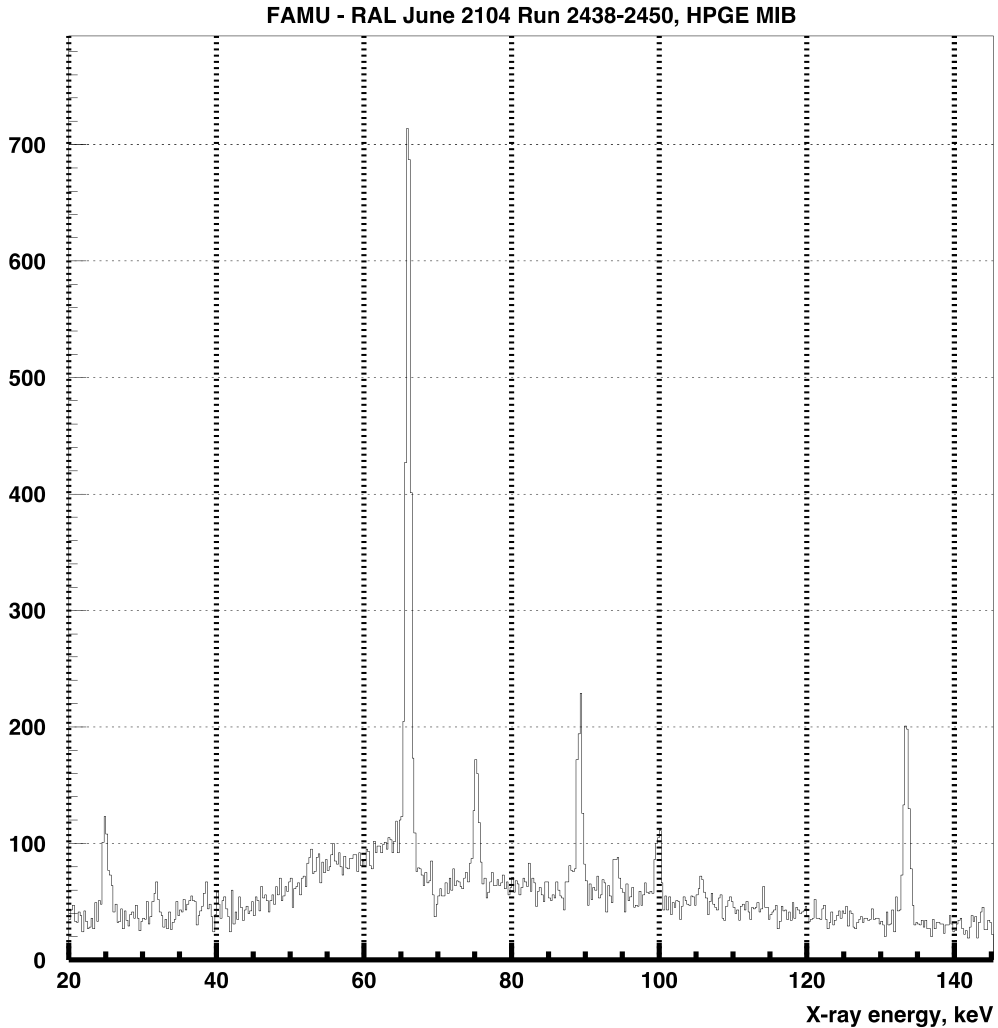

- 24.8 keV – O Lα
- 65.8 keV – Al Lα
- 75.2 keV – C Kα
- 89.2 keV – C Kβ
- (94.1 keV – C Kγ)
- 133.5 keV – O (2p-1s, Kα)

From preliminary data analysis:

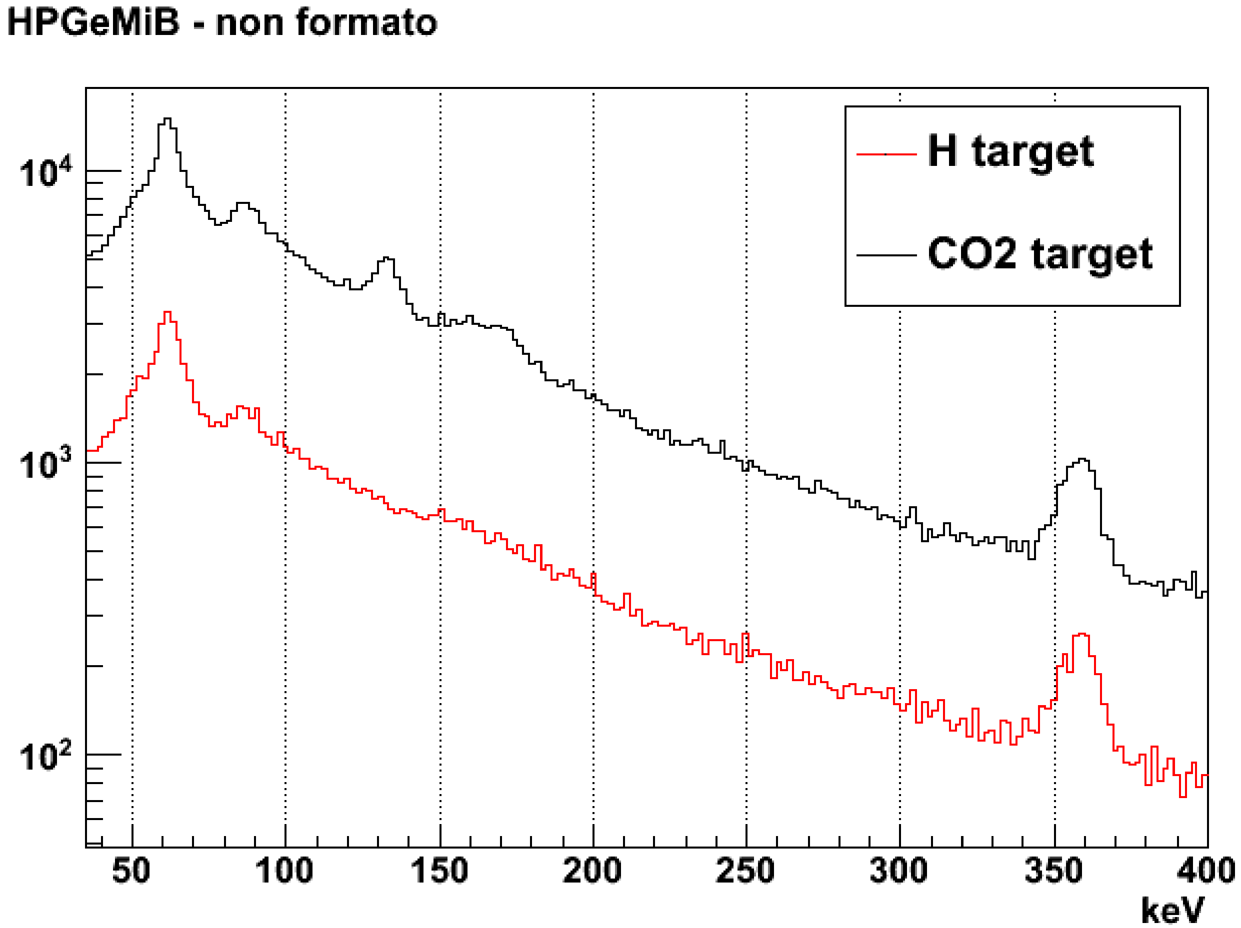

Monte Carlo simulations

Detailed simulations of every single process, incl. stopping, diffusion, depolarization, thermalization, muon transfer and decay of the μp atoms, and emission and propagation of characteristic X-rays.

Optimization of the target design and of the physical parameters (pressure, temperature, chemical composition, concentration) for the (1)muon transfer and (2)HFS experiments.

Incident muon beam (1)

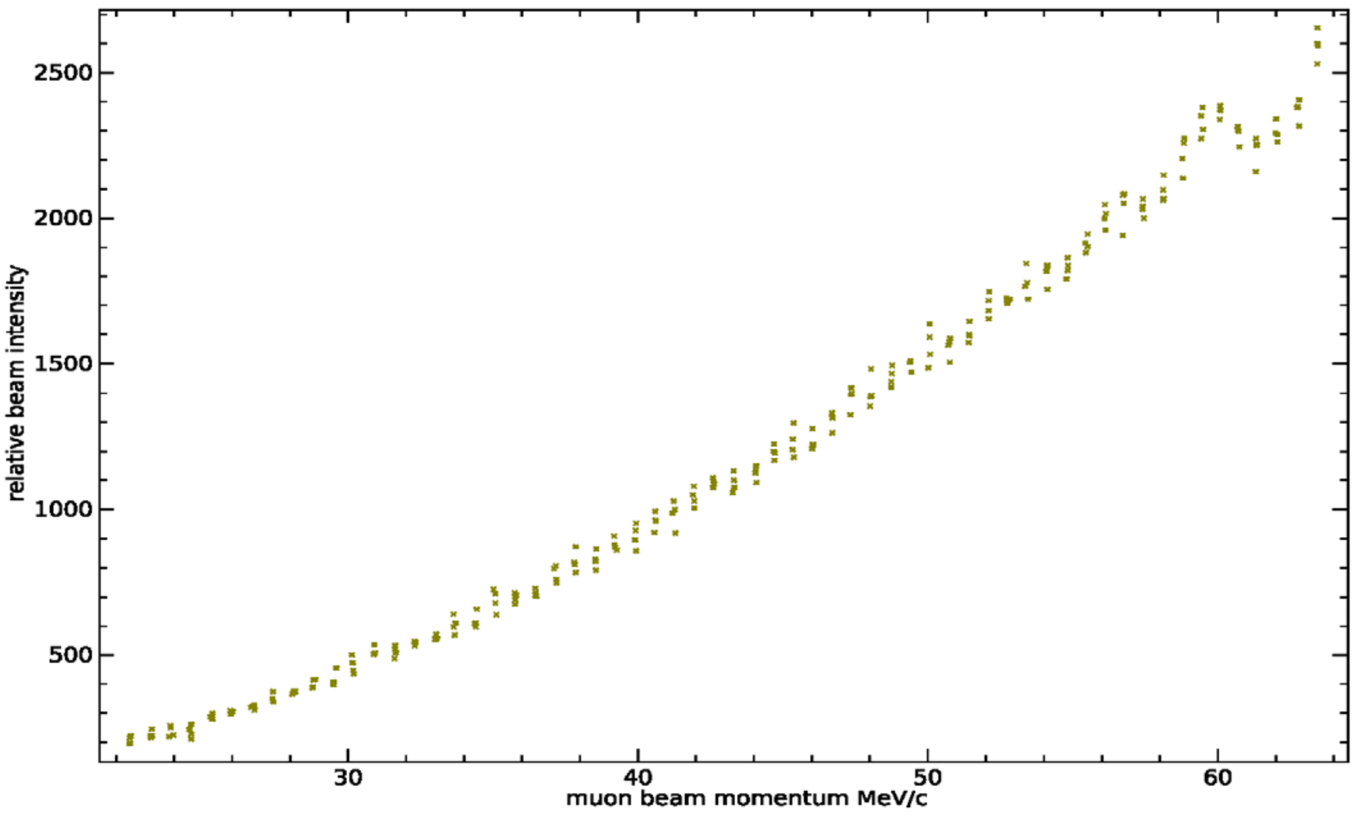

Stopping the muons

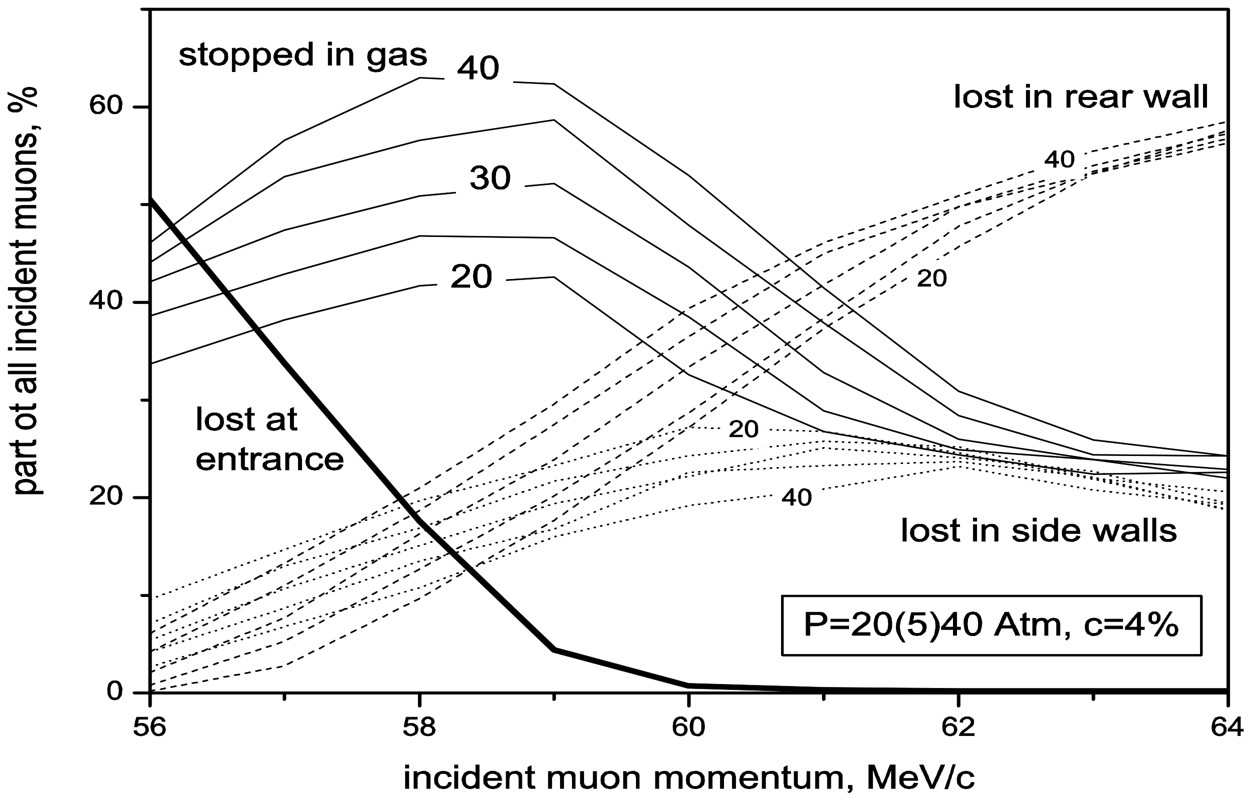

Stopping the muons (H_2+CO_2)

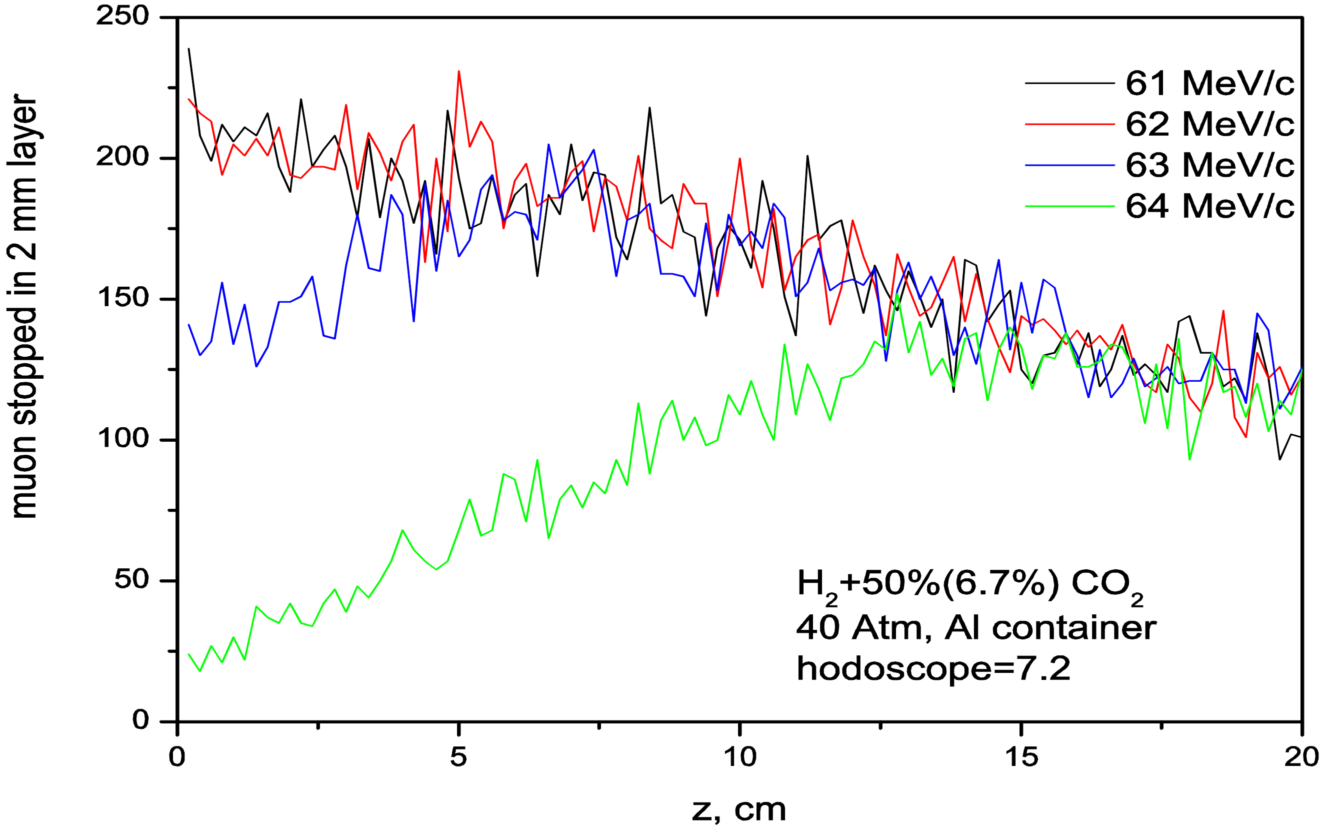

Stopping the muons (optimal)

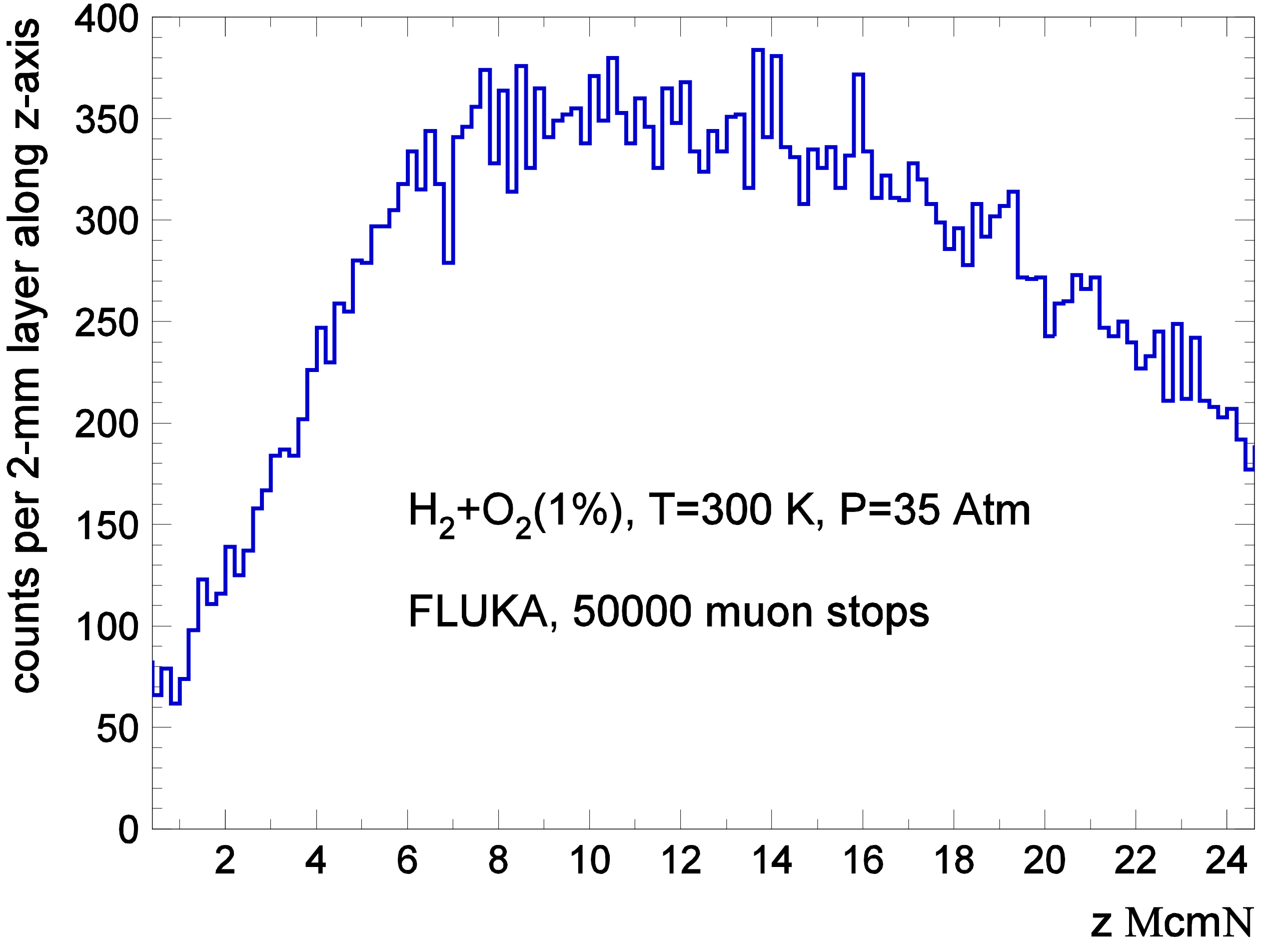

Optimization of O_2 concentration

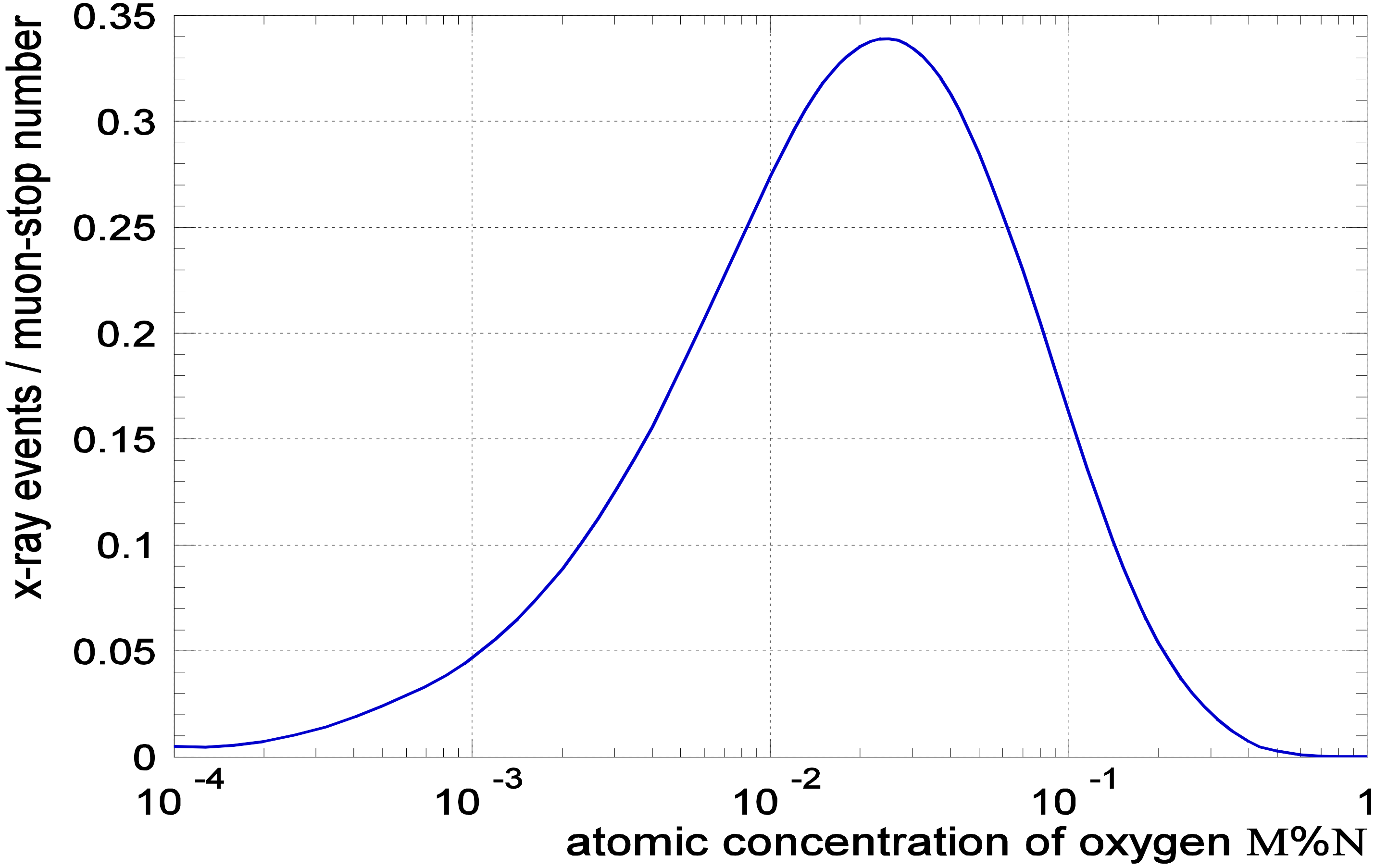

Transfer rate vs. temperature

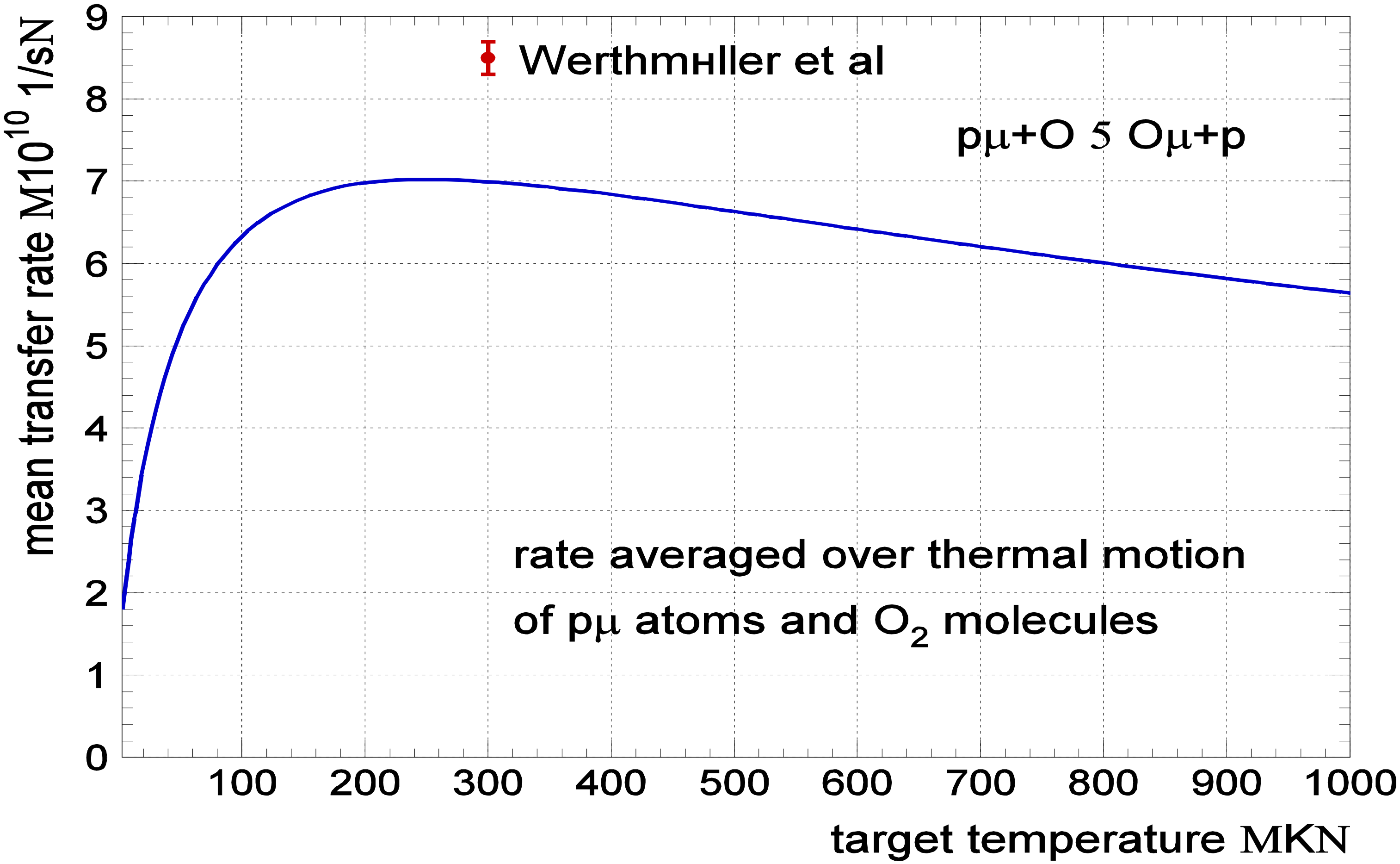

Old simulations of $\mu^{-}p$ HFS expt.

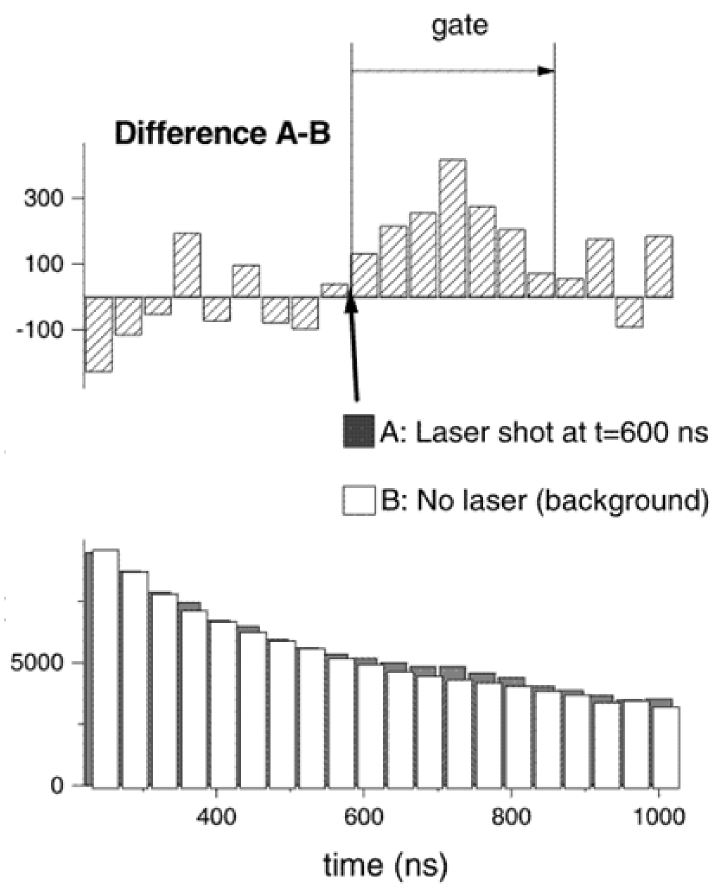

- The counts N_A, N_B in appropriately selected gate differ!
- Signal-to-noise ratio:

$$\rho = (N_A - N_B) / \sqrt{2(N_A + N_B)}$$

Achieved: $\rho \approx 10$

(subject to optimization)

P=10%

New simulations of μ⁻p HFS expt.

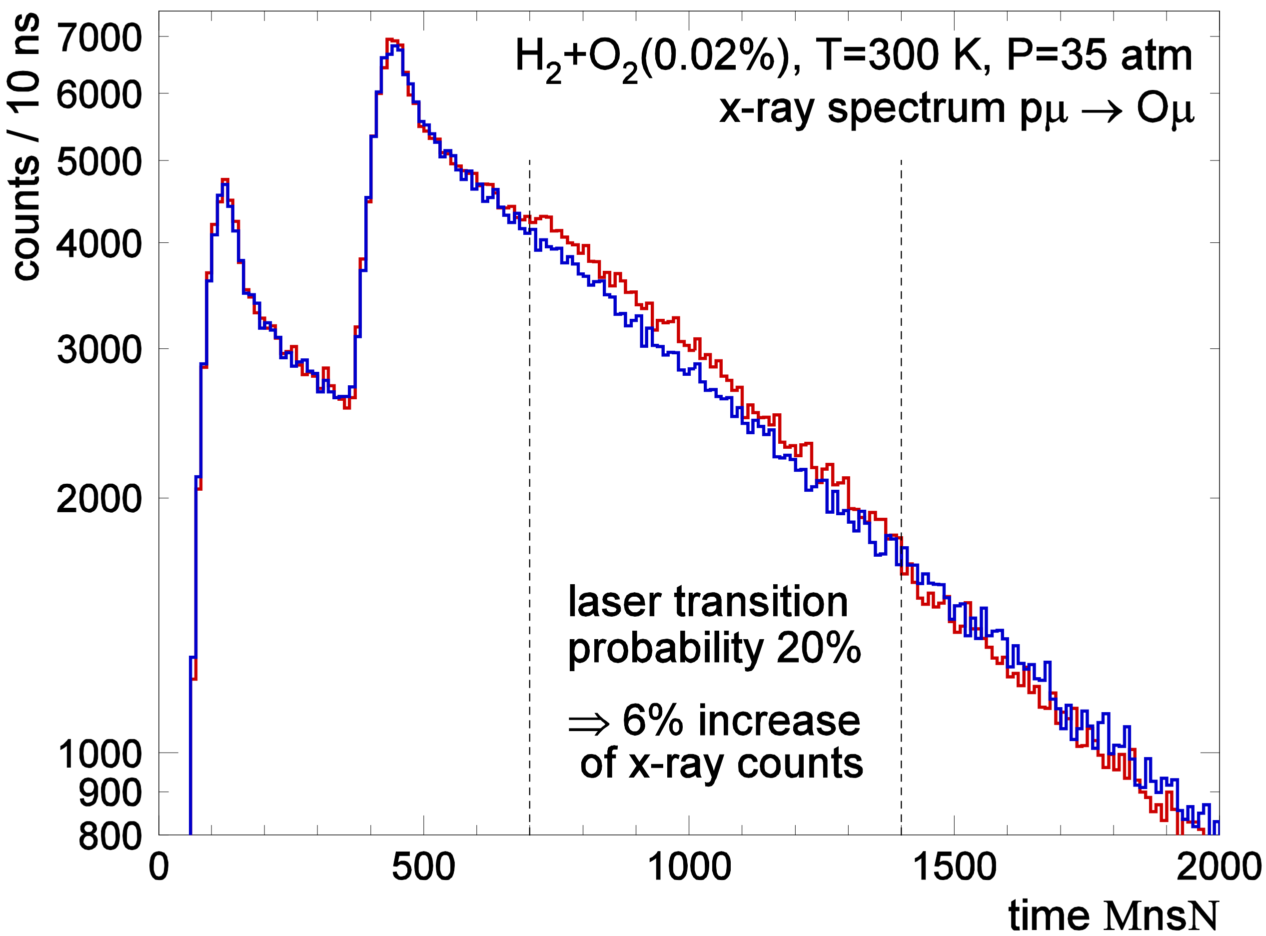

10^6 muonic atoms "shot", $\rho = 6\times10^4/\sqrt{4.10^6} = 30$.

Estimated laser efficiency

The spin-flip probability P is:

$$P = 0.2\ E/(S\sqrt{T})$$, where

E: pulse energy [J], S: laser beam cross section [cm^2]; T: temperature [K]

In a multipass cavity that provides n reflections, the irradiated volume by a 5mJ pulse at 30K is

$$V=(n.10^{-3}/P\sqrt{T})^{3/2}=7\ cm^3$$

for P=10%, T=30K, $n=2.10^3$

Estimated accuracy of resonance

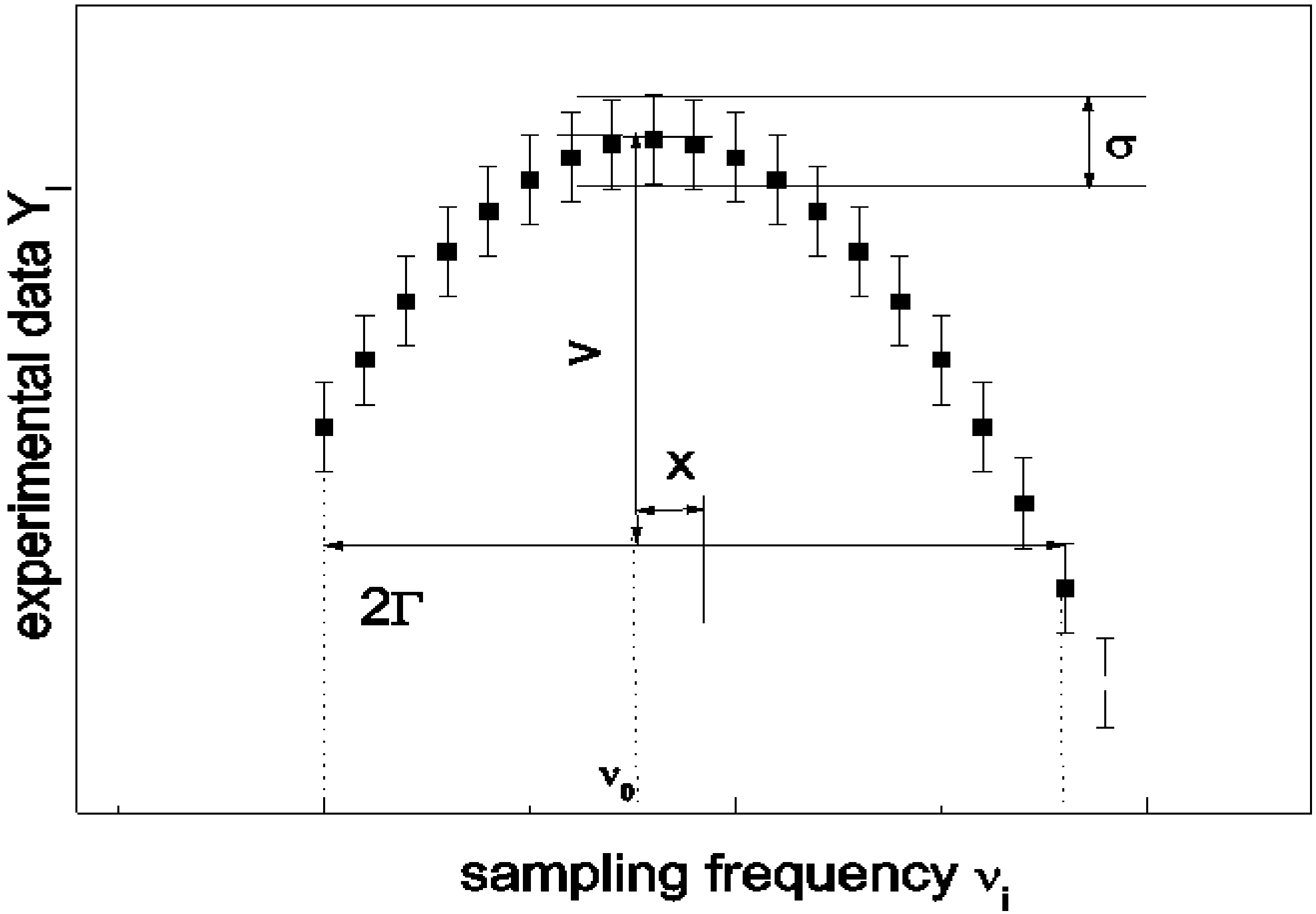

Estimated accuracy of the HFS expt.

$\delta\nu_0/\nu_0 \sim 0.2/(m^{1/2}\rho)(\Gamma/\nu_0)$ *[NIMB270(2012)]*

m: number of freq. samples; ρ: s/n ratio;
Γ: width of the investigated freq. interval

With 10^6 μ^- /sample, $\rho\sim 30$, m=10, the uncertainty reduction factor is

$$(\delta\nu_0/\nu_0) / (\Gamma/\nu_0) = 10^{-2}$$

and may be further improved.

Thank you!